

Elasto-plastic analysis using shell element considering geometric and material nonlinearities

N. Siva Prasad† and S. Sridhar‡

Department of Mechanical Engineering, Indian Institute of Technology, Madras-600 036, India

Abstract. An elasto-plastic finite element procedure using degenerated shell element with assumed strain field technique considering both material and geometric nonlinearities has been developed. This assumes von-Mises yield criterion, von-Karman strain displacement relations and isotropic hardening. A few numerical examples are presented to demonstrate the correctness and applicability of the method to different kinds of engineering problems. From present study, it is seen that there is a considerable improvement in the displacement value when both material and geometric nonlinearities are considered. An example of the spread of plastic zones for isotropic and anisotropic materials has been illustrated.

Key words: elasto-plastic; shell element; FEM; non-linear and Lagrangian in blank space.

1. Introduction

The classical degenerated shell elements produce over stiff solutions when applied to thin shell structures. This phenomena occurs due to shear and/or membrane locking (Pugh 1978, Zienkiewicz 1971). To eliminate the above locking problem, reduced and selective integration techniques are employed (Hinton, *et al.* 1978), but when coarse meshes are used the results are not reliable. Moreover spurious energy modes or mechanisms occur when lightly constrained boundaries are used which spread to all the elements resulting in incorrect solutions. To eliminate the above drawbacks (Huang and Hinton 1986), assumed strain field technique was used. In this reference, it was applied to problems with material nonlinearity but geometric nonlinearity was not considered. In many problems involving large displacements, it is essential to consider both geometric and material nonlinearity. In this paper, an attempt has been made to modify the Huang procedure to take care of both material and geometric nonlinearities. Numerical solutions have been obtained for example problems considering isotropic and anisotropic material properties. An example of spread of plastic zones for isotropic and anisotropic materials has been illustrated.

2. Finite element formulation of degenerated shell element

2.1. Assumptions

The assumptions made in the present procedure for a shell element, obtained from 3-D solid

† Professor

‡ Presently Research Scholar, deputed from CVRDE Avadi, Madras-600 054

element are given below.

- 1) Normals to the middle surface of the element before and after deformation remain straight.
- 2) Normal stress component in the thickness direction is zero and eliminated from the constitutive equations.

In the nodal point of a degenerated shell element there are three displacements u , v , w in the global x , y , z directions and two normal rotations β_1 and β_2 as shown in Fig. 1.

The basic formulations and notations have been followed in line with the reference (Huang and Hinton 1986) which gives the procedure for the elasto-plastic analysis using assumed strain field technique. In the present paper the following modifications have been carried out to incorporate the geometric nonlinearity.

2.2. Geometric nonlinearity

For the degenerated shell elements employed in this work a specific and appropriate Total Lagrangian formulation is adopted in which large deflection and moderate rotations (in the sense of von-Karman hypotheses) are accounted for. Hence the strain displacement relations in the local coordinate system are

$$\boldsymbol{\varepsilon} = \begin{Bmatrix} \varepsilon_x \\ \varepsilon_y \\ \gamma_{xy} \\ \gamma_{xz} \\ \gamma_{yz} \end{Bmatrix} = \begin{Bmatrix} \frac{\partial u'}{\partial x'} \\ \frac{\partial v'}{\partial y'} \\ \frac{\partial u'}{\partial y'} + \frac{\partial v'}{\partial x'} \\ \frac{\partial u'}{\partial z'} + \frac{\partial w'}{\partial x'} \\ \frac{\partial v'}{\partial z'} + \frac{\partial w'}{\partial y'} \end{Bmatrix} + \begin{Bmatrix} \frac{1}{2} \left(\frac{\partial w'}{\partial x'} \right)^2 \\ \frac{1}{2} \left(\frac{\partial w'}{\partial y'} \right)^2 \\ \left(\frac{\partial w'}{\partial x'} \right) \left(\frac{\partial w'}{\partial y'} \right) \\ 0 \\ 0 \end{Bmatrix} \quad (1)$$

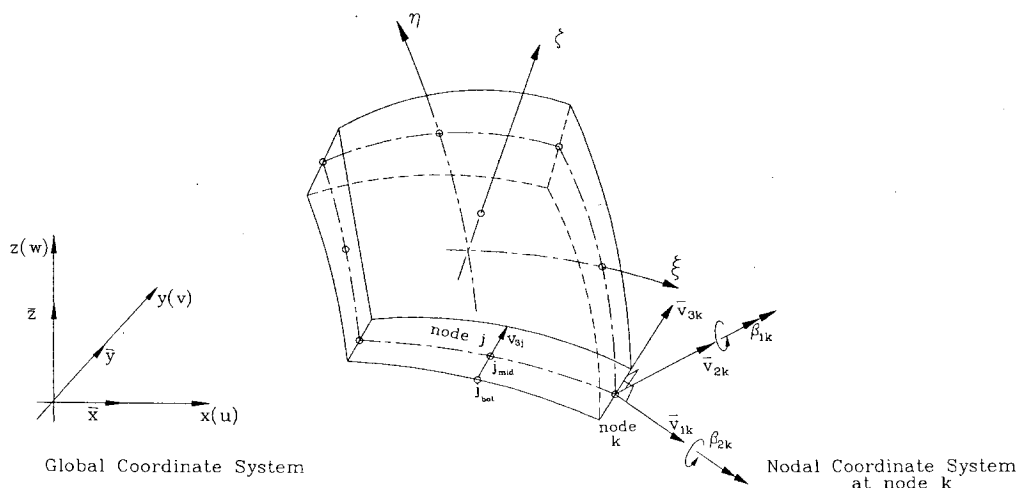


Fig. 1 Nodal and curvilinear systems for a degenerated shell element.

2.3. Elasto-plastic stress-strain relations

2.3.1. Elasticity matrix

The material is assumed to possess a state of anisotropy with three mutual orthogonal planes of symmetry. If the reference system of the orthogonal axis is parallel to the principal material axes, the stress strain relations are given by

$$\left. \begin{aligned} \epsilon_1 &= c_{11}\sigma_1 + c_{12}\sigma_2 + c_{13}\sigma_3 \\ \epsilon_2 &= c_{12}\sigma_1 + c_{22}\sigma_2 + c_{23}\sigma_3 \\ \epsilon_3 &= c_{13}\sigma_1 + c_{23}\sigma_2 + c_{33}\sigma_3 \\ \gamma_{12} &= c_{44}\tau_{12} \\ \gamma_{13} &= c_{55}\tau_{13} \\ \gamma_{23} &= c_{66}\tau_{23} \end{aligned} \right\} \quad (2)$$

where nine elastic constants C_{ij} can be expressed as functions of E , μ and G . For our case $\sigma_2 = \sigma_3 = 0$, and the elasticity matrix $[D]$ which relates stresses and strains, is given by

$$[D] = \begin{bmatrix} D_1 & D_{12} & 0 & 0 & 0 \\ D_{12} & D_2 & 0 & 0 & 0 \\ 0 & 0 & D_3 & 0 & 0 \\ 0 & 0 & 0 & D_4 & 0 \\ 0 & 0 & 0 & 0 & D_5 \end{bmatrix} \quad (3)$$

where

$$\begin{aligned} D_1 &= \frac{E_1}{(1 - \mu_{12}\mu_{21})} & D_2 &= \frac{E_2}{(1 - \mu_{12}\mu_{21})} & D_4 &= G_{13} \\ D_{12} &= \frac{E_2\mu_{12}}{(1 - \mu_{12}\mu_{21})} & D_3 &= G_{12} & D_5 &= G_{23} \end{aligned}$$

2.3.2. Huber-Mises yield criterion

The yield criterion used is of the form

$$\sigma^2 = a_1\sigma_1^2 + 2a_{12}\sigma_1\sigma_2 + a_2\sigma_2^2 + a_3\tau_{12}^2 + a_4\tau_{13}^2 + a_5\tau_{23}^2 \quad (4)$$

where a_1 , a_{12} , a_2 , a_3 , a_4 and a_5 are the anisotropic parameters.

2.3.3. Elasto-plastic matrix

The total strain increment ($d\epsilon$) is given by

$$d\epsilon = d\epsilon^e + d\epsilon^p \quad (5)$$

where $d\epsilon^e$ is the elastic component and $d\epsilon^p$ is the plastic component.

The plastic strain increment is given by

$$d\underline{\underline{\varepsilon}}^p = d\lambda \frac{\partial f}{\partial \underline{\underline{\sigma}}} \quad (6)$$

since we assumed associated plasticity theory. The elasto-plastic incremental strain relationship is given by

$$d\underline{\underline{\sigma}} = [D]_{ep} d\underline{\underline{\varepsilon}} \quad (7)$$

in which

$$[D]_{ep} = [D] - \frac{[D] \underline{\underline{a}} \underline{\underline{a}}^T [D]}{A + \underline{\underline{a}}^T [D] \underline{\underline{a}}} \quad (8)$$

and

$$\underline{\underline{a}}^T = \frac{\partial f}{\partial \underline{\underline{\sigma}}} \quad (9)$$

and A is the hardening parameter.

2.4. Solution procedure

During the general stage of the incremental/iterative solution of a finite element elasto-plastic problem the equilibrium equations will not be exactly satisfied and a system of residual forces $\underline{\underline{\psi}}$ will exist such that

$$\underline{\underline{\psi}}_i^n = \underline{\underline{f}}^n - \underline{\underline{p}}_i^n = \underline{\underline{f}}^n - \int_V \underline{\underline{B}}^T \underline{\underline{\sigma}}_i^n dV \neq 0 \quad (10)$$

in which $\underline{\underline{f}}$ and $\underline{\underline{p}}$ are respectively external applied force and internal equivalent force vectors, $\underline{\underline{B}}$ is the strain displacement matrix and $\underline{\underline{\sigma}}$ is the current stress field satisfying the yield condition, V denotes the volume of the solid, the superscript n signifies the load increment number, and subscript i the iteration cycle number within that increment. Taking the variation of Eq. (10) with respect to displacement $d\underline{\underline{a}}$, the tangential stiffness matrix for a geometrically non-linear problem is given by

$$\underline{\underline{K}} d\underline{\underline{a}} = d\underline{\underline{p}} = \int \underline{\underline{B}}^T d\underline{\underline{\sigma}} dV + \int d\underline{\underline{B}}^T \underline{\underline{\sigma}} dV \quad (11)$$

The strain displacement matrix $\underline{\underline{B}}$ may be separated into the usual part $\underline{\underline{B}}_o$ and non-linear contribution $\underline{\underline{B}}_L$ so that

$$\underline{\underline{B}} = \underline{\underline{B}}_o + \underline{\underline{B}}_L \quad (12)$$

Consequently $d\underline{\underline{B}}^T = d\underline{\underline{B}}_L^T$. Defining the initial stress or geometric stiffness $\underline{\underline{K}}_\sigma$ as

$$\underline{\underline{K}}_\sigma d\underline{\underline{a}} = \int (\underline{\underline{B}}_L^T \underline{\underline{\sigma}}) dV \quad (13)$$

$$\underline{\underline{K}} = \underline{\underline{\bar{K}}} + \underline{\underline{K}}_\sigma \quad (14)$$

in which

$$\bar{K} = \int \underline{B}^T \underline{D}_{ep} \underline{B} dV \quad (15)$$

where \underline{D}_{ep} is the elasto-plastic constitutive matrix.

From the Eq. (1),

$$\underline{\varepsilon} = \underline{\varepsilon}_o + \underline{\varepsilon}_L \quad (16)$$

where

$$\underline{\varepsilon}_L = \frac{1}{2} \underline{S} \underline{R} \quad (17)$$

where

$$\underline{S}^T = \begin{bmatrix} \frac{\partial w'}{\partial x'} & 0 & \frac{\partial w'}{\partial y'} & 0 & 0 \\ 0 & \frac{\partial w'}{\partial y'} & \frac{\partial w'}{\partial x'} & 0 & 0 \end{bmatrix} \quad (18)$$

and

$$\underline{R} = \begin{bmatrix} \frac{\partial w'}{\partial x'} \\ \frac{\partial w'}{\partial y'} \end{bmatrix} = \underline{G} \underline{a} \quad (19)$$

The term \underline{G} is a matrix with two rows and number of columns equal to the total number of element nodal variables.

Taking the variation of Eq. (17)

$$d\underline{\varepsilon}_L = \frac{1}{2} d\underline{S} \underline{R} + \frac{1}{2} \underline{S} d\underline{R} = \underline{S} \underline{G} d\underline{a} \quad (20)$$

and by definition we have

$$d\underline{B}_L = d\underline{S} \underline{G} \quad (21)$$

Also we have,

$$\underline{K}_\sigma d\underline{a} = \int_V \underline{G}^T d\underline{S}^T \underline{\sigma} dV \quad (22)$$

where

$$d\underline{S}^T \underline{\sigma} = [\underline{\sigma}] \underline{G} d\underline{a} \quad (23)$$

in which

$$[\underline{\sigma}] = \begin{bmatrix} \sigma_x & \tau_{xy} \\ \tau_{yx} & \sigma_y \end{bmatrix} \quad (24)$$

and hence

$$\underline{K}_\sigma = \int_V [\underline{G}]^T [\underline{\sigma}] [\underline{G}] dV \quad (25)$$

Using the above formulation and adopting the material non-linearity constitutive relations given in (Huang 1986) a finite element procedure is developed. A few numerical examples are given below to validate the above procedure.

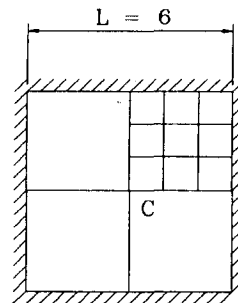
3. Numerical applications

The numerical results of the present method are compared with the reference (Hinton and Owen 1984). The computations are done using the program given in the reference (Hinton and Owen 1984) for accurate-numerical values, as published literature (Owen and Figueiras 1983) is in the form of graphs.

3.1. Clamped square plate subjected to concentrated load

Fig. 2(a) shows a clamped square plate subjected to a concentrated load at the centre. Due to its symmetry one quarter of the plate is discretized. In order to ascertain the convergence of the solutions, different mesh size are considered. Both isotropic and anisotropic material properties are taken into account and the displacements at final load step are tabulated in Table 1. The displacements are compared with (Owen, *et al.* 1983) and was found that the present analysis with assumed strain field technique gives better results even with coarse mesh when compared to the results obtained in the reference (Owen, *et al.* 1983).

The displacements at the centre for various load increments for isotropic and anisotropic cases is shown in Fig. 2(b).



THICKNESS = 0.2

MATERIAL PROPERTIES (UNITS MN, m)

Isotropic ;

$$E_x = E_y = 30 \times 10^3 \quad \nu = 0.3, \quad G_{xy} = G_{xz} = G_{yz} = 11540.0 \text{ p.s.i.}$$

$$\bar{\sigma}_0 = \sigma_{0x} = \sigma_{0y} = \sigma_{045} = 30.0$$

$$\tau_{012} = \tau_{013} = \tau_{023} = 17.32$$

$$\bar{E}_p = E_{px} = E_{py} = E_{pz} = 300 \quad G_p = 100.0$$

Anisotropic ;

$$\alpha_y = 40.0 \quad \alpha_{45} = 35.0 \quad \tau_{012} = 20.20$$

Remaining values are same as for the Isotropic case

Fig. 2(a) Clamped square plate subjected to concentrated load at center.

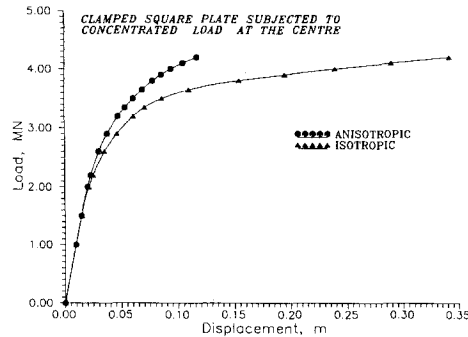
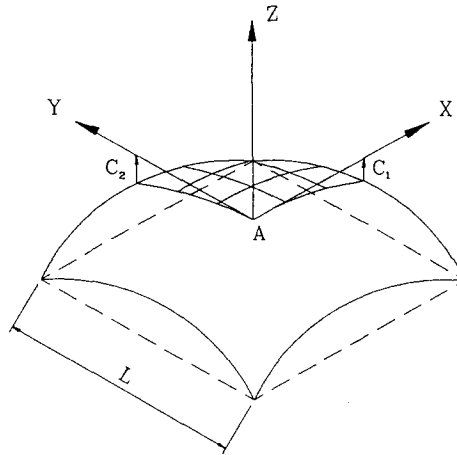


Fig. 2(b) Load vs vertical displacement at centre.

3.2. Clamped quadratic shell subjected to concentrated load at the centre

An elasto-plastic analysis of a clamped quadratic shell subjected to concentrated load at its centre is taken. The material properties and geometric characteristics are given in Fig. 3(a). Different meshes are used to study the variation in the displacements. The displacement at the centre for various load increments for isotropic and anisotropic cases is shown in Fig. 3(b). Displacements at final load step are compared with that of (Owen, *et al.* 1983), and (Huang, *et al.* 1986) and are tabulated in Table 2. It is found that with the present analysis there is an improvement in results compared to semiloof thin formulation.



GEOMETRIC CHARACTERISTICS

$$C = C_1 = C_2 = \frac{L}{10}$$

$$Z = \frac{C}{(L/2)^2} (X^2 + Y^2)$$

THICKNESS = 0.20

MATERIAL PROPERTIES
SAME AS IN EXAMPLE 1

Fig. 3(a) Clamped quadratic shell with concentrated load at center.

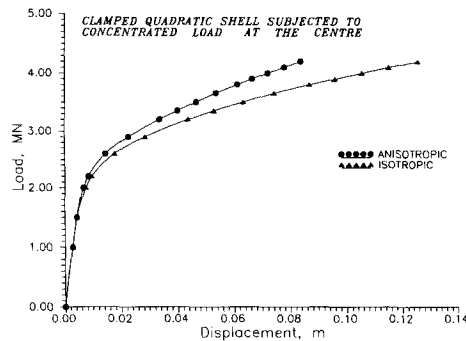


Fig. 3(b) Load vs vertical displacement at centre.

In Fig. 3(c), the plastic zone distributions are shown in quarter of the shell for the final load step. The difference between the isotropic and anisotropic material behaviours are highlighted by considering the intensity of the plastic strain. A lack of symmetry is seen in the distribution of plastic zones for the anisotropic case.

To obtain the above results for a mesh size of 6×6 , the computational time taken for the present analysis is 35 minutes, on a PC 486 with 8 MB RAM. Compared to the Hinton and Owen method, saving in the computational time is 170 per cent on the same system with the present method.

3.3. Cylindrical shell subjected to self weight

The classical example of the cylindrical shell roof shown in Fig. 4(a) subjected to self weight loading is considered. The isotropic results obtained with the present analysis is compared with the exact deep shell solution (Huang, *et al.* 1986) and found to be in excellent agreement. The displacements at final load step for different mesh sizes considering both isotropic and anisotropic material characteristics are tabulated in Table 3. The displacements at the centre for various load

Table 1 Clamped square plate subjected to concentrated load at the centre

Mesh size	Deflection, <i>m</i>			
	Isotropic		Anisotropic	
	Present	Owen	Present	Owen
3×3	-0.002859	-0.001923	-0.002859	-0.001923
4×4	-0.196000	-0.089281	-0.071220	-0.064280
6×6	-0.341000	-0.194000	-0.136600	-0.1261000

Table 2 Clamped quadratic shell subjected to concentrated load at the centre

Mesh Size	Deflection, <i>m</i>					
	Isotropic				Anisotropic	
	Present with GNL	Haung	Owen with GNL	Owen without GNL	Present	Owen with GNL
3×3	-0.05618	-0.05584	-0.06548	-0.06467	-0.02339	-0.03649
4×4	-0.09235	-0.09124	-0.17990	-0.10627	-0.05034	-0.08727
6×6	-0.12580	-0.12366	-0.22760	-0.20761	-0.08385	-0.12540

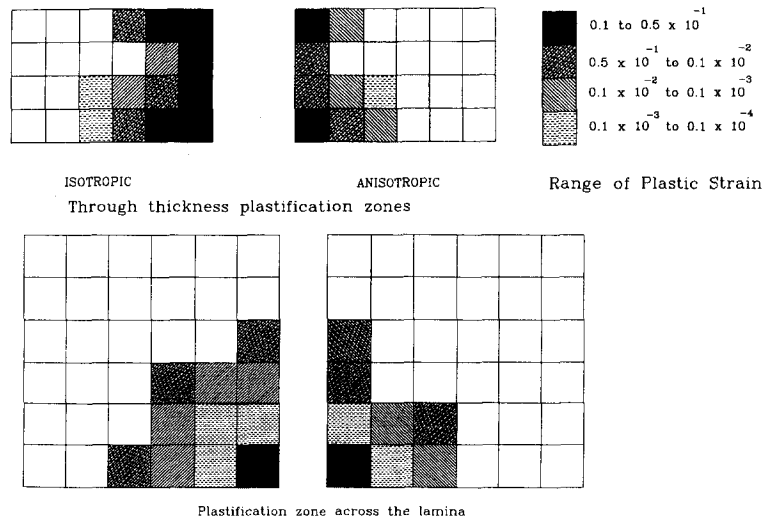
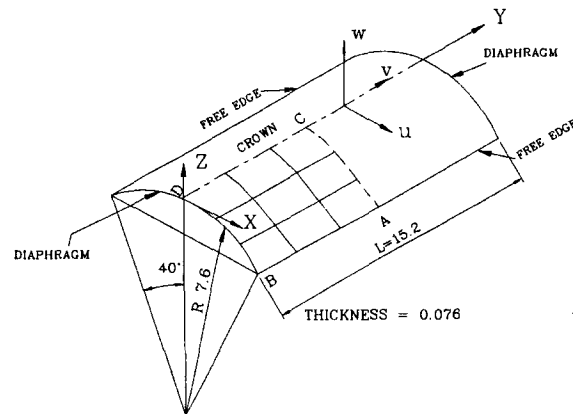


Fig. 3(c) Camped quadratic shell under central point load-spread of plastic zones.



MATERIAL PROPERTIES (UNITS MN, m)

ISOTROPIC

$$E_1 = E_2 = 21000$$

$$G_{12} = G_{13} = G_{23} = 10500$$

$$\sigma_0 = \sigma_1 = \sigma_2 = \sigma_3 = 4.1$$

$$\tau_{12} = \tau_{21} = \tau_{13} = 2.367$$

$$E_p = G_p = 0.0$$

ANISOTROPIC

$\sigma_1 = 2\sigma_0$ REMAINING VALUES ARE THE SAME AS FOR THE ISOTROPIC CASE

Fig. 4(a) Cylindrical roof configuration.

increments for isotropic and anisotropic material conditions are shown in Fig. 4(b).

4. Conclusions

The elasto-plastic analysis using assumed strain field degenerated shell element for both thick and thin isotropic and anisotropic shells and plates taking into account the geometric and material nonlinearities is carried out. Numerical examples have been presented and the dis-

Table 3 Cylindrical shell subjected to self weight

Mesh size	Present analysis				Exact deep shell solution	
	Deflection, <i>m</i>					
	Isotropic		Anisotropic		Isotropic	
	at <i>C</i> *	at <i>A</i> *	at <i>C</i>	at <i>A</i>	at <i>C</i>	at <i>A</i>
3 × 3	0.0124	− 0.0797	0.0123	− 0.0791		
4 × 4	0.0131	− 0.0855	0.0130	− 0.0848	0.0137	− 0.0917
6 × 6	0.0139	− 0.0921	0.0136	− 0.0907		

*C and A are the locations as shown in the Fig. 4(a).

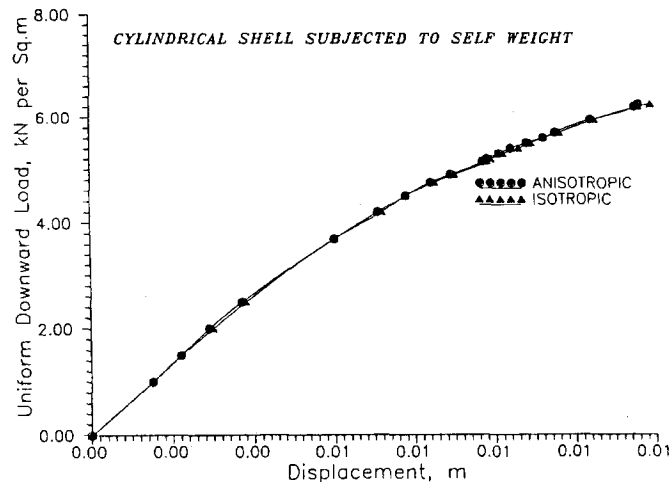


Fig. 4(b) Load vs vertical displacement at centre.

placement values show that the present analysis gives better results compared to that of values reported in literature. An unsymmetric spread of plastic zones across the lamina has occurred for anisotropic case and it is symmetric for isotropic case. The analysis establishes the improvement in results by considering the geometric and material nonlinearity together while applying to appropriate engineering problems.

References

- Bathe, K.J. and Dvorkin, E.N. (1985), "A four-node plate bending element based on Mindlin/Reissner plate theory and a mixed, interpolation", *Int. J. Numer. Meth. Engng.*, **21**, 367-383.
- Hinton, E. and Owen, D.R.J. (1984), "Finite element software for plates and shells", Pineridge Press Ltd.
- Huang, H.C. (1987), "Membrane locking and assumed strain shell elements", *Comput. and Struct.*, **27**, 671-677.
- Huang, H.C. (1987), "Implementation of assumed strain degenerated shell elements", *Comput. and Struct.*, **25**, 147-155.
- Huang, H.C. and Hinton, E. (1984), "A nine node lagrangian mindlin, plate element with enhanced shear interpolation", *Eng. Comput.*, **1**, 369-379.
- Huang, H.C. and Hinton, E. (1986), "A new nine-node degenerated, shell element with enhanced membrane and shear interpolation", *Int. J Numer. Meth. Engng.*, **22**, 73-92.
- Huang, H.C. (1989), "Static and dynamic analysis of plates and shells: theory, software and applications",

Springer-Verlag.

- Owen, D.R.J. and Figueiras, J.A. (1983), "Anisotropic elasto-plastic finite element analysis of thick and thin plates and shells", *Int. J Numer. Meth. Engng.*, **19**, 541-566.
- Owen, D.R.J. and Figueiras, J.A. (1983), "Elasto plastic analysis of anisotropic plates and shells by the semiloof element", *Int. J Numer. Meth. Engng.*, **19**, 73-92.
- Pugh, E.D.L., Hinton, E. and Zienkiewicz, O.C. (1978), "A study of quadilateral plate bending element with reduced integration", *Int. J Numer. Meth. Engng.*, **12**, 1059-1079.
- Zienkiewicz, O.C., Taylor, R.J. and Too, J.M. (1971), "Reduced integration techniques in general analysis of plates and shells", *Int. J Numer. Meth. Engng.*, **3**, 275-290.

Notations

\underline{a}	displacement vector
$\underline{B}, \underline{B}_o, \underline{B}_L$	strain displacement matrices
\underline{D}_{ep}	elasto-plastic constitutive matrix
$\underline{K}, \underline{K}_\sigma$	total stiffness and geometric stiffness matrices respectively
u, v, w	global displacements
u', v', w'	local displacements
V	volume of the domain
x, y, z	global cartesian coordinates
x', y', z'	local cartesian coordinates
β_1, β_2	normal rotation
ε	von-Karman strain
σ	2nd Piola-Kirchhoff stress
$\underline{\psi}, \underline{f}, \underline{p}$	residual, external applied force and internal equivalent force vectors, respectively
$\underline{\xi}, \underline{\eta}, \underline{\zeta}$	natural curvilinear coordinates